THE ASTROPHYSICAL JOURNAL, 387:56–68, 1992 March 1


# THE SNAPSHOT SURVEY: A SEARCH FOR GRAVITATIONALLY LENSED QUASARS WITH THE *HUBBLE SPACE TELESCOPE*[1]

J. N. BAHCALL,[2] D. MAOZ,[2,3] R. DOXSEY,[4] D. P. SCHNEIDER,[2,3] N. A. BAHCALL,[5] O. LAHAV,[6] AND B. YANNY[2]

*Received 1991 May 6; accepted 1991 September 9*

## ABSTRACT

In a systematic attempt to find new examples of multiply imaged quasars that are the result of gravitational lensing, 89 short exposures, through two filters, of high-luminosity quasars from a well-defined sample have been obtained with the *Hubble Space Telecope*'s Planetary Camera. Useful high-resolution images of approximately 30 quasars have resulted. None of the quasars show evidence of multiple images due to gravitational lensing. Simulations show that multiple images with brightness ratios of up to several magnitudes would have been detected, down to image separations of $\approx 0\overset{''}{.}1$. These results are compared with lower resolution ground-based surveys and current theoretical predictions. The Snapshot Survey has uncovered several engineering problems in the observatory's performance, some of which have already been corrected. In particular, we find that the large telescope pointing errors and drift rates are primarily the result of the lack of correction for stellar aberration when pointing and tracking are performed solely with gyroscopes. The implications of the possibly low intrinsic gyro drift rate on future observations are briefly discussed.

*Subject headings:* gravitational lensing — quasars: general — telescopes

## 1. INTRODUCTION

This paper presents initial results from the *Hubble Space Telescope* (*HST*) Non-Proprietary Snapshot Survey. In its current incarnation, the Snapshot Survey is an imaging survey of bright quasars using *HST*'s Planetary Camera (PC). Short exposures (2 or 4 minutes) are taken during gaps in the scheduled observing program, when the telescope would otherwise be idle. Snapshot targets are assigned only after all other programs have been scheduled. All images are obtained using only the gyroscopes for pointing and guiding, thus saving the time necessary to acquire guide stars. Targets are distributed throughout the sky, so only short slews (typically a few degrees) are required to move the telescope from any approved science target to a nearby Snapshot target. In principle, the Snapshot survey could encompass any set of scientifically interesting objects that are distributed on the sky with a sufficiently large surface density. The data are non-proprietary and can be obtained from the Space Telescope Science Institute's (STScI) User Support Branch.

The scientific purpose of the currently operating Snapshot Survey is to search for evidence of gravitational lensing among known distant, intrinsically luminous quasars. Despite the spherical aberration of HST's primary mirror, the sharp core of the point-spread function, containing $\sim 15\%$ of the light, permits high spatial resolution studies of closely separated bright point sources (Burrows et al. 1991). The existing point-spread function permits the detection of multiple images at subarcsecond separations, which cannot be easily probed from the ground (see § 4).

Theoretical lensing models (e.g., Turner, Ostriker, & Gott 1984, hereafter TOG) predict that many gravitationally lensed quasars have multiple images with these small separations and have therefore not yet been resolved from the ground. Recent estimates (Kochanek 1991; Fukugita & Turner 1991, hereafter FT) suggest that one-half of all gravitationally lensed quasars have subarcsecond image separations. Large uncertainties exist in the predicted frequency of quasar lensing by galaxies, due to uncertainties concerning galactic potentials, galaxy luminosity functions and evolution, the relation of velocity dispersion to luminosity, the distribution of galaxy types, the intrinsic (unlensed) quasar number-magnitude relation, and observational selection effects.

Gott, Park, & Lee (1989), Fukugita, Futamese, & Kasai (1990), and Turner (1990) have noted that the predicted rate of lensing is also strongly dependent on some cosmological parameters, allowing the observed rate of lensing to place interesting contraints on cosmological models. Kochanek (1991) has argued that existing catalogs of optically selected quasars may discriminate against lensed quasars, because at the typical image separations of a few arcseconds, a lensed quasar would not satisfy the requirement that an object be pointlike in appearance to be included in a survey. Similarly, a quasar that is lensed by a galaxy may also be reddened by it and as a result may not pass the color criteria of UV-excess surveys. He cites the small number of three-image configurations versus five-image configurations among known lensed quasars as evidence for severe incompleteness of existing quasar surveys or, alternatively, a fundamental problem with the theoretical models. FT and Fukugita et al. (1991) claim that, despite the uncertainties in the various parameters, the small number of known lensed quasars argues against the existence of a flat universe dominated by a cosmological constant. This is important in view of the recent renewed interest in cosmologies dominated by a cosmological constant, invoked to solve a number of fundamental problems (see, e.g., Lahav et al. 1991).

[1] Based on observations with the NASA/ESA *Hubble Space Telescope*, obtained at the Space Telescope Science Institute, which is operated by the Association of Universities for Research in Astronomy, Inc., under NASA contract NAS5-26555.

[2] Institute for Advanced Study, Princeton, NJ 08540.

[3] Guest Investigator, Palomar Observatory, California Institute of Technology.

[4] Space Telescope Science Institute, 3700 San Martin Drive, Baltimore, MD 21218.

[5] Princeton University Observatory, Princeton, NJ 08544.

[6] Institute of Astronomy, Madingley Road, Cambridge CB3 0HA, England.

A number of ground-based searches for gravitationally lensed quasars have been performed. The results vary greatly in the fraction of lens candidates reported. Crampton et al. (1989) observed 32 quasars with a high-resolution camera and classified seven of them as gravitational-lens candidates. Surdej (1989) and Meylan & Djorgovski (1989) are carrying out imaging surveys of bright quasars from catalogs and have classified 23% of 111 objects observed as "interesting" and possibly lensed. None of the 33 $z > 3$ quasars of Schneider, Schmidt, & Gunn (1991) display any signatures of lensing at scales of 1″.5. Webster et al. (1988) and Fugmann (1988) have found a large excess of foreground galaxies around quasars and invoked amplification by lensing to explain the effect, again suggesting that a large fraction of quasars is gravitationally lensed. A similar conclusion was reached by Stocke et al. (1987) who found that X-ray-selected quasars are typically more distant when in the neighborhood of a foreground galaxy. Searches for gravitational lenses with large ($>2''$) image separations are being carried out at Cambridge using automated scanning of Schmidt plates (Webster, Hewett, & Irwin 1988). VLA imaging of quasars from the MIT–Greenbank radio survey (Bennett et al. 1984) has turned up cases of gravitational lensing of radio-loud quasars.

To resolve the conflicting reports on the frequency of lensing of quasars, there are several advantages to searching for multiple images in the range of separations down to 0″.1. This range includes practically all expected cases of quasars multiply lensed by galaxies. As mentioned above, about half of the lensing cases are expected to have subarcsecond separations, which will appear pointlike in ground-based surveys. At these small separations, the probabilty of chance superpositions of unrelated objects is small, especially if the Galactic plane is avoided. While some of the surveys are sensitive to subarcsecond structure, detection of subarcsecond multiple images from the ground relies on some form of image reconstruction (deconvolution, PSF subtraction) that may introduce uncertainties that are difficult to quantify. The scientific purpose of the current version of the Snapshot Survey is to determine the statistics of small-separation gravitational lensing.

In addition to the study of gravitational lensing, the Snapshot Survey data monitor the performance of *HST* on gyros, and thus provide valuable engineering data. Toward this goal, we have measured the gyro drift rate and pointing error on each exposure.

Section 2, below, describes the sample. The observations are presented in § 3. Section 4 analyzes the engineering data. Section 5 describes the scientific results. The main conclusions are discussed in § 6.

## 2. SAMPLE DEFINITION

The quasar catalog of Véron-Cetty & Véron (1987) was used to construct the Snapshot Survey sample. The criteria for inclusion were a redshift greater than 1 based on a slit spectrum, an absolute magnitude $M_V$ brighter than $-25.5$, and Galactic latitude $|b| > 10°$. Absolute magnitudes were calculated using a Hubble constant of $H_0 = 100$ km s$^{-1}$ Mpc$^{-1}$, decceleration parameter $q_0 = 0.5$, $k$-corrections assuming an optical power-law spectral index of $-0.5$, and Galactic absorption corrections from de Vaucouleurs, de Vaucouleurs, & Corwin (1976). The selections in redshift and absolute magnitude were made in order to increase the probability of including lensed quasars in the sample (e.g., TOG). The Galactic latitude restriction reduces the chance of having bright foreground stars on the field of view (see below). In addition, we thus avoid crowded stellar fields, where chance superpositions of foreground objects are more likely, and minimize the Galactic absorption correction.

A fixed constraint, required in order to ensure that Snapshot exposures do not interfere with subsequent exposures, was the absence of bright stars near the quasar. If an object is excessively overexposed in the PC, then a "residual image" (Griffiths 1990) of the source will appear in subsequent exposures. Residual images occur in the PC CCDs when a pixel receives $\approx 200$ times the analog saturation number of 32,000 photoelectrons. For the most sensitive filter we use, F555W, the number of pixels containing residual images can be calculated from the expression $N = T \times 10^{0.4(8.21 - V)}$, where $V$ is the apparent visual magnitude and $T$ is the exposure time in seconds. We included in the sample only quasars for which nearby bright stars would cause less than $3 \times 10^{-4}$ of the total pixels to have residual images in the specified exposure time. This was determined by calculating the number of "supersaturated" pixels resulting from all *HST* guide stars within 120″ of the quasar. This restriction removed about 10% of the quasars from the sample.

To avoid overlap with previously approved *HST* science programs, we also required that the quasar not be included in any accepted *HST* imaging program. This requirement removed 32 sources. Of these, five quasars (0142−100, 0957+561, 1115+080, 1413+117, and 2237+0305) are previously known cases of gravitational lensing, and their elimination must be taken into account in subsequent calculation of the lensing statistics of our sample. Our final sample thus consists of 354 quasars. Since the targets are located all over the sky, relatively short slews are required between a given science target and the nearest Snapshot object. We display in Figure 1 the distribution of angular separations between approved Cycle 1 *HST* science targets and the nearest Snapshot target. The average angular distance to the nearest Snapshot target is 10°. We have provided STScI with software that automatically matches each primary science target with the Snapshot targets which require the least telescope motion. However, in the early commissioning period discussed here, *HST* scheduling has not routinely made use of this software; for the observations presented here, large slews were frequently used.

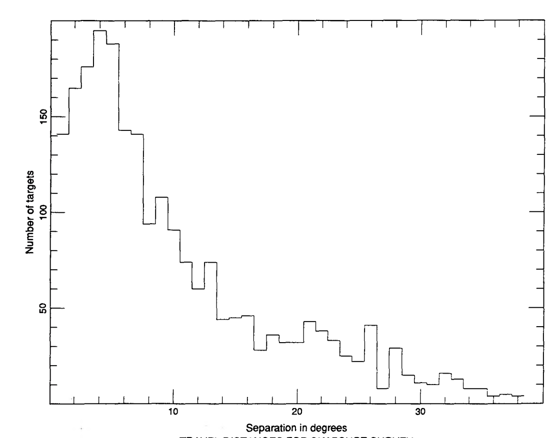


FIG. 1.—Distribution of distances between *HST*-approved Cycle 1 targets and the nearest Snapshot Survey object.

## 3. *HST* OBSERVATIONS

The observations were carried out under *HST* proposals 3034, which was active from 1990 September 17 to 1991 January 4, and 3092, which was active from 1990 December 30 to 1991 March 29. All of the observations were taken with the Planetary Camera (see Griffiths 1990 for a detailed description of this instrument). The PC consists of four 800 × 800 Texas Instruments CCDs arranged in a 2 × 2 mosaic. The image scale is 0"043 pixel$^{-1}$, and each CCD covers a field 34" on a side. Proposal 3034 consisted of 120 exposures with the object centered on CCD 7 of the PC. (The four CCDs of the PC are designated as PC-5 through PC-8). The F555W and F785LP filters were used (hereafter $V$ and $I$, respectively). Proposal 3092 consisted of 230 s exposures with the object at the (10, 10) position on PC-7 (i.e., displaced from the center of the CCD mosaic 10" in the column direction and 10" in the row direction) through the same filters. Except for two observations (see § 5, below), all exposures used only gyro guiding. A number of objects were observed more than once in the same filter because of scheduling difficulties in the initial stages of operation.

The observations are listed chronologically in Table 1 (proposal 3034) and Table 2 (proposal 3092). The drift rate for each exposure was determined by measuring the length of the trail of the quasar or of stars in the field of view. Finally, we list the telescope's pointing error, or, in cases where we could not identify the field of view, a lower limit on the error. Table 3 lists the results obtained for each observation in order of the right ascension of the targets. Figure 2 shows some typical exposures with the two filters used, with a variety of object brightnesses and trail lengths.

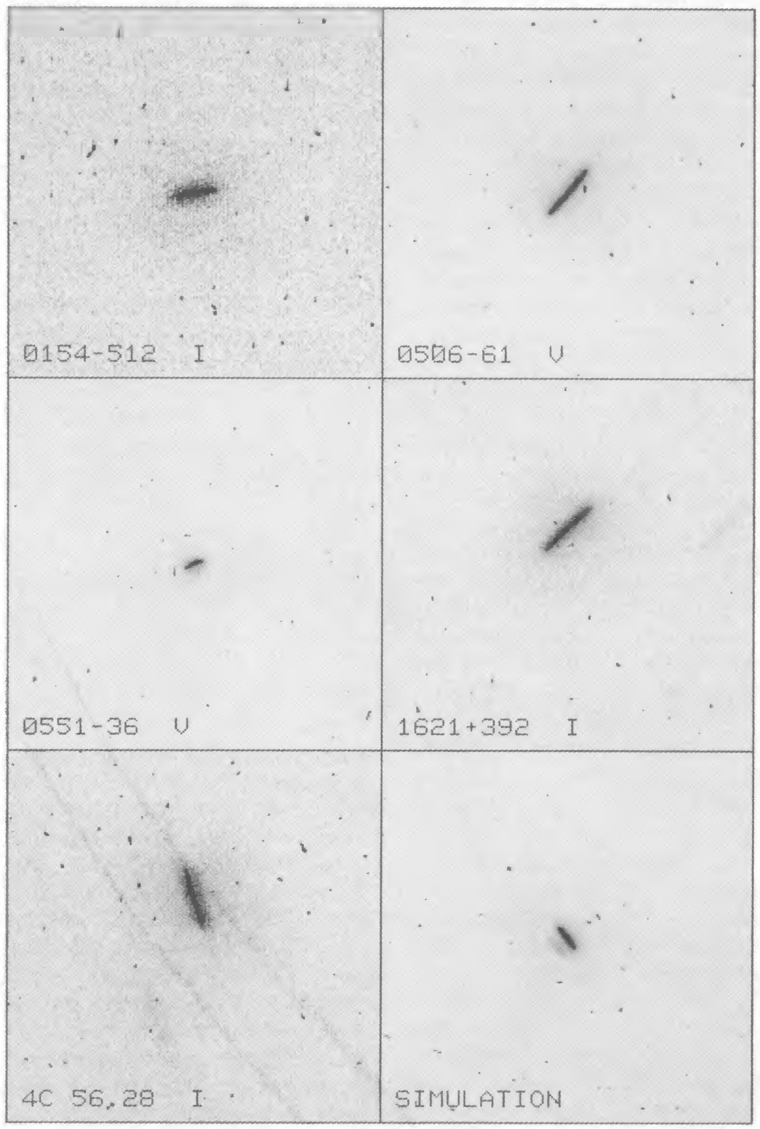


FIG. 2.—Segments of typical Planetary Camera exposures of five Snapshot Survey quasars, with a variety of brightnesses and trail lengths. The image scale is 0"043 pixel$^{-1}$, and the field for each panel is 8"6 on a side. The orientation of the images is random, according to the *HST* roll angle at the time of the exposure. The gray scale is set individually for each image, such that the darkest hue corresponds to the number of counts pixel$^{-1}$ in the brightest part of the quasar. The numerous dark specks in the images are charged-particle events. The filter used is indicated following the object name ($V$ for F555W, and $I$ for F785LP). The lower right-hand panel shows a simulated image of a quasar and a secondary image 2 mag fainter, separated by 0"3. The primary image corresponds to a 17th mag object trailed at a rate of 4.6 mas s$^{-1}$ in the 120 s exposures, or a 17.8 mag object trailed at a rate of 2.4 mas s$^{-1}$ in the 230 s exposures.

TABLE 1

OBSERVATIONS: 17 SEPTEMBER 1990 TO 4 JANUARY 1991

| Date (UT) | Object and Filter | | Trail Rate (mas/sec) | Pos. Error (arcsec) | Comments |
|---|---|---|---|---|---|
| 091790 | 0014+81 | V | – | >18 | Empty field. |
| " | 0014+81 | I | 5.0 | 10 | |
| " | 0355–48 | V | 6.0 | 12 | Identification uncertain; possibly larger error. |
| 091890 | 0149+33 | V | 3.0 | 16 | Identification uncertain; possibly larger error. |
| 091990 | 0149+33 | I | 4.0 | 37 | |
| " | 0201+36 | V | 5.5 | 36 | |
| " | 0355–48 | I | – | >18 | Empty field. |
| 092090 | 0201+36 | I | 2.7 | 31 | |
| " | 0225–014 | V | 3.0 | 45 | |
| " | 0225–014 | I | 3.0 | 20 | Identification uncertain; possibly larger error. |
| 100190 | 0451–418 | V | 3.7 | >18 | Identification uncertain. |
| " | 0451–418 | I | 3.6 | >18 | |
| 100390 | 0506–61 | V | 4.6 | 18 | |
| " | 0506–61 | I | 5.2 | 26 | |
| " | 0551–366 | V | 5.5 | 6 | |
| 100490 | 0551–366 | I | 5.0 | 23 | |
| " | 0743–67 | V | 5.5 | 11 | |
| " | 0743–67 | I | 4.2 | 15 | |
| " | 1039+81 | V | 5.5 | >18 | Identification uncertain. |
| 100690 | 1039+81 | I | 5.0 | >18 | Identification uncertain. |
| 100990 | 1711+712 | I | 4.0 | 14 | |
| 101190 | 1345+58 | V | 4.3 | 25 | 4C58.27 |
| " | 1345+58 | I | 4.5 | 20 | 4C58.27 |
| " | 1613.7+1715 | V | 4.9 | 10 | |
| " | 1613.7+1715 | I | 3.7 | 7 | |
| " | 1704+710 | V | 5.0 | 7 | |
| " | 1704+710 | I | 5.3 | 8 | |
| " | 1711+712 | V | 4.0 | 12 | |
| 101290 | 2150+05 | V | – | >18 | Empty field. |
| " | 2150+05 | I | 4.5 | 12 | Identification uncertain; possibly larger error. |
| 110590 | 0014+81 | I | 1.8 | 0.8 | Guided observation (coarse track). |
| 010491 | 0014+81 | V | 1.0 | 60 | 2nd guided observation, but target not in field. |

NOTE.—Proposal ID 3034: 120 s exposures with object centered on PC-7. A software problem with the positioning command was discovered and corrected toward the end of these observations. The two filters used are abbreviated as *V* (F555W) and *I* (F785LP). The listing is chronological.

## 4. ENGINEERING RESULTS

It was apparent from the start of the program that large pointing errors were being made (see Table 1). In many exposures, the target was located outside the field of view. Often the quasar appeared on the wrong CCD, or very near the edge. In addition, the images were degraded by drift rates about 4 times larger than preflight expectations.

The average drift rate for the period covered in Table 1 was $4.5 \pm 0.9$ mas $s^{-1}$ (milliarcseconds second$^{-1}$), where the quoted error is the rms dispersion. The drift rate ranged from 2.7 to 6.0 mas $s^{-1}$, with a median value of 4.5 mas $s^{-1}$. The median pointing error during this period is about 20″, and the mean pointing error was probably close to 30″. In approximately one-half of the exposures, the targets did not appear anywhere on the PC.

In an attempt to find the source of the large pointing errors, we helped uncover a software error which caused a misplacement of the targets relative to their intended location. The position was displaced by 14″. This error was corrected by the STScI toward the end of the period covered by Table 1. We also discovered a software error that set the drift rate equal to zero after a slew (i.e., ignoring information from previous guided exposures). This was corrected for observations starting 1990 October 9 but did not significantly improve the gyro drift rate.

The average drift rate during the period covered by Table 2 was $4.3 \pm 1.4$ mas $s^{-1}$. The measured drift rate ranged from 0.6 to 7.2 mas $s^{-1}$, with a median value of 4.3 mas $s^{-1}$. There is no significant difference in the average drift rate between 1990 September–December and 1991 January–March. The median pointing error for the observations in Table 2 is 21″. In about one-third of the second set of exposures, the target was not placed anywhere on the PC. The modest improvement in the pointing error between Table 1 and Table 2 is consistent with

TABLE 2

OBSERVATIONS: 30 DECEMBER 1990 TO 29 MARCH 1991

| Date (UT) | Object and Filter | | Trail Rate (mas/sec) | Pos. Error (arcsec) | Comments |
|---|---|---|---|---|---|
| 123090 | 0743−67 | V | 4.9 | 9 | |
| " | 1148−00 | V | – | >24 | Empty field. |
| 010891 | 0743−67 | V | 4.7 | 10 | |
| 010991 | 0506−61 | V | 5.7 | 22 | |
| 011091 | 0743−67 | I | 4.3 | 14 | |
| 011191 | 0034+39 | V | 6.6 | 24 | 5C03.44 |
| 020491 | 0051+29 | I | 4.1 | 4 | |
| " | 0154−512 | I | 3.0 | >24 | |
| " | 0039−03 | I | 4.0 | 5 | UM666 |
| 020691 | 0145+38 | I | 3.2 | 3 | |
| 020791 | 0039−03 | V | 4.3 | 5 | UM666 |
| 020891 | 0014+81 | I | 3.9 | 15 | |
| " | 0034+39 | I | 3.0 | 9 | 5C03.44 |
| 021291 | 0051+29 | V | 3.0 | >24 | |
| 021791 | 0014+81 | V | 2.0 | 15 | Trail is very curved and uneven. |
| " | 0145+38 | V | 4.4 | 60 | |
| " | 0153+74 | V | 6.0 | 15 | |
| " | 0153+74 | I | 3.0 | 9 | |
| " | 0154−512 | V | 3.4 | 23 | |
| " | 0146−500 | V | 6.6 | >24 | |
| " | 0146−500 | I | 5.6 | 7 | |
| 021891 | 0514−16 | V | 5.8 | 20 | |
| " | 0514−16 | I | 4.7 | 22 | |
| " | 0551−36 | V | 1.7 | 22 | |
| " | 0551−36 | I | 2.3 | 21 | |
| " | 1621+392 | V | 4.3 | >24 | |
| " | 1621+392 | I | 6.0 | 15 | |
| " | 1857+56 | V | 3.7 | 60 | Coordinates 4C56.28 |
| 022091 | 1718+481 | V | 5.0 | 15 | |
| " | 1718+481 | I | 1.3 | 8 | |
| 022291 | 1857+56 | I | 5.3 | 24 | 4C56.28 |
| 022591 | 0149+33 | V | 4.0 | 9 | |
| " | 0149+33 | I | 5.2 | 11 | |
| " | 0326+27 | V | – | >24 | Empty field. |
| " | 0326+27 | I | – | >24 | Empty field. |
| 022791 | 0822+27 | I | 6.4 | 18 | Identification uncertain; error could be larger. |
| " | 0819−032 | V | 2.8 | 90 | |
| 022891 | 0421+019 | V | – | >24 | Empty Field. |
| 030191 | 0421+019 | I | 3.0 | 35 | |
| " | 0348+06 | V | 0.6 | 17 | |
| 030391 | 0348+61 | I | 5.8 | 18 | |
| 030891 | 0454+039 | V | – | >24 | Empty Field |
| " | 0454+039 | I | 2.8 | 6 | Identification uncertain; error could be larger. |
| " | 0749+37 | V | 5.2 | 15 | |
| " | 0749+37 | I | 4.8 | 13 | |
| " | 0822+27 | V | 4.7 | 21 | |
| " | 0506−61 | I | 5.6 | 24 | |
| " | 0642−5038 | V | 7.2 | 40 | |
| " | 0642−5038 | I | 5.0 | 53 | |
| 030991 | 0308+1902 | V | 4.0 | 23 | |
| " | 0308+1902 | I | 3.8 | 22 | |
| 031291 | 0819−032 | I | 4.3 | 13 | |
| " | 1021−00 | I | 4.3 | 20 | |
| 031691 | 1039+81 | I | 5.6 | >24 | |
| 032791 | 1039+81 | V | 4.4 | 22 | |
| 032891 | 0836+71 | V | – | >24 | Empty field. |
| 032991 | 0836+71 | I | 5.3 | >24 | |

NOTE.—Proposal ID 3092: 230 s exposures; target positioned on PC-7 14″ from the apex. The two filters used are abbreviated as $V$ (F555W) and $I$ (F785LP). The listing is chronological.

TABLE 3

SUMMARY OF SNAPSHOT SURVEY

| Quasar | Filter | CCDs on which objects appear | Trail (mas/sec) | Comments |
|---|---|---|---|---|
| 0014+81 | V | none | – | Target missed. |
| | I | 7 | 5 | Object in PC-7 is likely to be the quasar, judging from the in a repeated observation (see below). The apparently double trail (0.15″ separation) is a PSF artifact. |
| | I | 7,8,8 | 1.8 | Quasar on PC-7. Guided observation (coarse track) for comparison with unguided previous observation. |
| | V | 8,8 | <1 | Quasar not in field view. 2nd guided observation, as above. Probable identification of this pair of stars suggests the quasar was 1' SW of the center of PC-7. |
| | I | 7,7,7 | 3.9 | Quasar is the object fully inside the PC-. |
| | V | 5,5,7,7 | 2 | Quasar on edge of PC-7. Trail is very curved and uneven. |
| 5C03.44 | V | 5,6,6,8 | 6.6 | Quasar near corner of PC- 8. |
| | I | 5,6,7 | 3.0 | Quasar in PC-7. |
| UM666 | I | 7,7,7 | 4.0 | Quasar is brighter object in PC-7. |
| | V | 7 | 4.3 | Likely the quasar on PC- 7. |
| 0051+29 | I | 6,7 | 4.1 | Quasar likely on PC-7; faint PC-6 object not on POSS. |
| | V | 7 | 3 | Target missed. Only some very faint object on PC-7. |
| 0145+38 | I | 5,6,7 | 3.2 | Quasar on PC-7; PC-5 object barely on POSS. |
| | V | 5,6 | 4.4 | Target missed. PC-6 star is 50″ south of quasar, which is 60″ off PC-7. |
| 0146−500 | V | 7 | 6.6 | Very faint. Target missed. |
| | I | 7 | 5.6 | Likely the quasar. |
| 0149+33 | V | 7 | <3 | Possibly the quasar. |
| | I | 7,8 | 4 | PC-8 object could be quasar; faint object on POSS at separation of PC-7 object. |
| | V | 6,6,7 | 4.0 | Quasar on PC-7. |
| | I | 5,6,6,7 | 5.2 | Quasar on PC-7. Trail perpendicular to that in preceeding V exposure. |
| 0153+74 | V | 5,6,7,7 | 6.0 | Quasar is object nearer to apex on PC-7. |
| | I | 5,5,6,4x7,8 | 3.0 | Quasar in PC-7 (same objects as above, and some more). Trail perp. to previous exposure. |
| 0154−512 | I | 5,6,7,7 | 3.4 | Fainter PC-7 object is quasar. |
| | V | 7,7 | 6.8 | Fainter object on edge of PC-7 is quasar. |
| 0201+36 | V | 7,8 | 5.5 | Probably pair of stars to SW of quasar; quasar missed by 20″. |
| | I | 7 | 2.7 | Probably same star as on PC-7 in the V exposure. Quasar missed by 15″. |
| 0225−01 | I | 7,5 | <3 | Object on PC-7 faint and near edge; object on PC-5 may be quasar; if so, position off by 45″. |
| | V | 7 | 3 | Faint and near edge; unclear if hit/miss. |
| 0308+1902 | V | 6,7 | 4.0 | Quasar on PC-7. (Faint PC-6 object not on POSS). |
| | I | 5,6,6,7,7 | 3.8 | Quasar on PC-7. (All other faint objects not on POSS). |
| 0326+27 | V | none | – | Empty field. |
| | I | none | – | Empty field. |

TABLE 3—*Continued*

| Quasar | Filter | CCDs on which objects appear | Trail (mas/sec) | Comments |
|---|---|---|---|---|
| 0348+06 | V | 7 | 0.6 | Quasar in PC-7, judging by counts and expected emptiness of field. |
| | I | 7,7 | 5.8 | Same as above. Very faint PC-7 object not on POSS. |
| 0355−48 | V | 6 | 6 | Possibly the quasar. |
| | I | none | – | Target missed. |
| 0421+019 | V | none | – | Empty Field. |
| | I | 5,6,6 | 3.0 | Stars to south of quasar, at POSS limit. Target missed by 35″. |
| 0451−418 | V | 5 | 3.7 | Possibly the quasar. |
| | I | 7 | 3.6 | Probably a star; too bright to be the quasar. |
| 0454+039 | V | none | – | Empty Field. |
| | I | 5,7,7 | 2.8 | Uncertain whether brighter PC-7 object is quasar; fainter objects not on POSS. |
| 0506−61 | V | 6,7,8 | 4.6 | PC-7 object is the quasar. |
| | I | 5,5,6 | 5.2 | Quasar missed by 10″. One and a half stars from previous frame of the same object included. |
| | V | 5,5,6,6,7,8 | 5.7 | Brighter PC-6 object is quasar. Trail North-South, as in previous V exp. |
| | I | 3x5,2x6,2x8 | 5.6 | Faint stars and galaxies to SE of quasar. Quasar missed by 24″. |
| 0514−16 | V | 5,5,5,7-8 | 5.8 | Quasar split between PC-s 7 and 8. |
| | I | 5,5,5,8 | 4.7 | Quasar in PC-8 (same objects as in previous exposure). |
| 0551−36 | V | 6,7,7,7 | 5.5 | PC-7 object near apex almost certainly quasar. |
| | I | 6,7,8 | 5 | Target missed. |
| | V | 5,8,8 | 1.7 | Quasar is fainter PC-8 object. |
| | I | 5,8,8,8 | 2.3 | Quasar in PC-8 (same configuration as previous exp., but trail perp.). |
| 0642−5038 | V | 5,6,6,7,7,8 | 7.2 | Stars to SE of quasar. Quasar missed by 40″. |
| | I | 5,5,7 | 5.0 | Same stars as in PC-s 7 and 8, above. Quasar missed by 53″. |
| 0743−67 | V | 7,7,8 | 5.5 | Bright PC-7 object is quasar. |
| | I | 7,7,7 | 4.2 | Quasar in PC-7 (same 3 objects as in previous exposure). |
| | V | 5,5,7,7 | 4.9 | Quasar in PC-7 (bright). "Secondary" component 0.7″ NW of quasar is most probably just PSF halo. |
| | V | 5,5,7,7,7 | 4.7 | Quasar in PC-7 (bright). |
| | I | 7,8 | 4.7 | Quasar in PC-7. |
| 0749+37 | V | 7 | 5.2 | Probably the quasar, although 1 magnitude fainter than expected. |
| | I | 7 | 4.8 | Probably the quasar, although 1 magnitude fainter than expected. |
| 0819−032 | V | 5,5,6,6 | 2.8 | Target missed by 90″. Stars to west of quasar. |
| | I | 5,5,5,7,7,7 | 4.3 | Quasar is faint object near center of PC-7. |
| 0822+27 | I | 7 | 6.4 | PC-7 object very faint; quasar either faded or missed. |
| | V | 7 | 4.7 | Apparently the same object as in the preceeding I exposure. Probably the quasar is 1 magnitude fainter than expected. |
| 0836+71 | V | none | – | Empty field. |
| | I | 6 | 5.3 | Object 2 to 3 mag fainter than expected for the quasar. Probable miss. |
| 1021−00 | I | 6, 7 | 4.3 | Quasar in PC-7. |
| 1039+81 | V | 5,6 | 5.5 | Quasar probably missed. |
| | I | 6 | 5 | Identification uncertain. |
| | I | 6, 8 | 5.6 | Target missed. Very faint, diffuse object on PC-8. |

TABLE 3—*Continued*

| Quasar | Filter | CCDs on which objects appear | Trail (mas/sec) | Comments |
|---|---|---|---|---|
| | V | 6,7,8 | 4.4 | Quasar on PC-7. 1.5 mag fainter than object in previous I exposure, indicating that one was missed. |
| 1148−00 | V | none | – | Target missed. |
| 4C58.27 | V | 6,8 | 4.3 | Quasar on PC-6. Barred spiral galaxy on PC-8. |
| | I | 7,8 | 4-5 | Quasar on PC-7, but very near edge, very faint. Spheroid of galaxy on PC-8. |
| 1613.7+1715 | V | 7 | 4.9 | Likely to be quasar (judging from counts and expected emptiness of field). |
| | I | 5,7 | 3.7 | Likely to be quasar on PC-7. Faint PC-5 object not on POSS. |
| 1621+392 | V | 7 | 4.3 | Target missed. |
| | I | 5,7,7,7,8 | 6.0 | Quasar in PC-7, plus 2 additional stellar-like images 7.2″ west and 3.6″ east of it, too faint to be seen on POSS. |
| 1704+710 | V | 5,7,8 | 5 | Quasar on PC-7. |
| | I | " | 5.3 | Quasar on PC-7. |
| 1711+712 | I | 6,7 | 4 | Possibly quasar on PC-7. Faint (diffuse?) object on PC-6, not on POSS. |
| | V | 6,7 | 4 | Same as previous exposure. |
| 1718+481 | V | 7,8 | 5.0 | Quasar in PC-7. |
| | I | 7,8,8,8 | 1.3 | Quasar in PC-7. Trail short and perp. to previous exposure. |
| 4C56.28 | V | 6,8 | 3.7 | Target missed. Probably stars to south and south-east of quasar. |
| | I | 8,8,8 | 5.3 | Quasar is fainter PC-8 object. Additional object 2.7″ SE of it. |
| 2150+05 | V | none | – | Target missed. |
| | I | 6,6,6,7 | 4.5 | Uncertain identification; faint objects not on POSS. |

NOTE.—$V$ = F555W, $I$ = F785LP, POSS = Palomar Sky Survey, PSF = point-spread function.

what would be expected from correcting the offset error in the positioning command mentioned above, if the intrinsic pointing error was indeed $\approx 25''$.

In response to the large pointing errors and drift rates, a number of possible explanations were investigated. We have determined that stellar aberration corrections are not applied in the current control system when *HST* is operating solely on gyros. The stellar aberration due to the motion of Earth around the Sun is

$$\theta = \frac{v}{c} \sin \phi = 20\overset{''}{.}5 \sin \phi , \tag{1}$$

where $v$ is Earth's velocity around the Sun, $c$ is the speed of light, and $\phi$ is the angle between Earth's velocity vector and the direction of the object being observed. The orbital motion of *HST* about Earth contributes an additional aberration term with an amplitude of 5″. The spacecraft's centripetal acceleration around Earth will cause the object's position to drift at a rate

$$\frac{d\theta}{dt} = \frac{1}{c} \frac{dv}{dt} \sin \theta \approx 5.5 \sin \theta \text{ mas s}^{-1} , \tag{2}$$

where $\theta$ is the angle between the spacecraft's acceleration vector and the direction of the object.

Comparing these relations to the observations above, we see that the lack of stellar aberration correction can account for much of the pointing error and of the drift rate. To test this hypothesis, we examined the relation between the *HST* direction of motion relative to the target direction and the drift rate for several individual exposures. As expected, the cases of large gyro drifts correspond approximately to motion toward the target, and the smaller drift rates correspond approximately to perpendicular motion.

Since the pointing error is occasionally larger than can be explained by stellar aberration alone, other effects must also be at work. Since 1991 April, the *HST* operation procedures have been modified to invoke the on-board stellar aberration corrections for observations carried out under gyro control. We will continue to monitor the performance of the gyros throughout *HST*'s Cycle 1 of observations.

## 5. SCIENCE RESULTS

A total of 89 exposures of 38 quasars have been obtained, through the $V$ and/or $I$ filters. Due to the poor pointing performance, we cannot be certain that an object appearing in the field of view is the targeted quasar unless other objects appear which permit the identification of the field of view. In some cases, there is only one stellar object on the exposure, and no other objects are expected to be seen in the field of view if the observed stellar object were the quasar. Due to this ambiguity,

TABLE 4

OBSERVED QUASARS

| Object | $z$ | $V$ | $M_V$ | Comments |
|---|---|---|---|---|
| 0014+81 | 3.41 | 16.5 | -28.16 | |
| 5C03.44 | 1.94 | 17.95 | -25.62 | |
| UM666 | 2.74 | 18.5 | -25.74 | |
| 0051+29 | 1.83 | 17.8 | -25.65 | Likely observed. |
| 0145+38 | 1.44 | 16.0 | -26.98 | |
| 0146-500 | 2.26 | 18.3 | -25.57 | Likely observed. |
| 0149+33 | 2.43 | 18.5 | -25.51 | |
| 0153+74 | 2.34 | 16.0 | -27.94 | Observed $V = 18.0$. |
| 0154-512 | 1.66 | 17.3 | -25.96 | |
| 0225-014 | 2.04 | 18.15 | -25.52 | Identification uncertain. Observed $V = 19.0$. |
| 0308+1902 | 2.84 | 18.6 | -25.71 | Likely observed. |
| 0348+06 | 2.06 | 17.6 | -26.09 | Likely observed. Observed $V = 18.0$. |
| 0355-48 | 1.02 | 16.38 | -25.89 | Identification uncertain. Observed $V = 16.8$. |
| 0451-418 | 2.13 | 18.2 | -25.55 | Identification uncertain. |
| 0454+039 | 1.35 | 16.53 | -26.31 | Identification uncertain. |
| 0506-61 | 1.09 | 16.85 | -25.57 | Observed $V$ =17.4 to 18.5. |
| 0514-16 | 1.28 | 16.95 | -25.79 | |
| 0551-36 | 2.32 | 17.57 | -26.35 | |
| 0743-67 | 1.51* | 16.37 | -26.70 | Observed $V = 16.9$. |
| 0749+37 | 1.20 | 16.5 | -26.11 | Likely observed. Observed $V = 18.1$. |
| 0819-032 | 2.35 | 18.2 | -25.75 | |
| 0822+27 | 2.06 | 17.7 | -25.99 | Likely observed. Observed $V = 18.9$. |
| 1021-00 | 2.55 | 18.53 | -25.57 | |
| 1039+81 | 1.26 | 16.5 | -26.21 | Observed $V = 18.2$. |
| 4C58.27 | 2.04 | 17.5 | -26.17 | |
| 1613.7+1715 | 2.73 | 18.5 | -25.74 | |
| 1621+392 | 1.97 | 17.5 | -26.10 | |
| 1704+710 | 2.00 | 17.5 | -26.13 | |
| 1711+712 | 1.60 | 17.5 | -25.69 | Likely observed. |
| 1718+481 | 1.08 | 14.71 | -27.69 | |
| 4C56.28 | 1.60 | 17.3 | -25.88 | |
| 2150+05 | 1.98 | 17.77 | -25.84 | Identification uncertain. |

* This quasar's redshift is erroneously revised in Hewitt & Burbidge 1989 to $z = 0.395$. This was the redshift reported by Tritton 1971. Jauncey et al. 1989 found that $z = 1.512$, as assumed here.

we cannot say precisely how many quasars have been successfully observed. The degree of this uncertainty is indicated in Table 3 for each observation. Of the 38 quasars observed, 20 are confirmed to be in the field of view in at least one exposure by the presence of other known objects. An additional seven quasars are likely to have been imaged. The likely cases are those for which no other stars are expected to be in the field of view, and/or the observed magnitude of the quasar is consistent with that expected. Six quasars were definitely missed in all their attempted exposures. The observations of the remaining five quasars are inconclusive, as indicated in Table 3.

Table 4 lists the 32 quasars that were observed or possibly observed in at least one exposure. Also tabulated is their redshift and $V$ magnitude (from Véron-Cetty & Véron 1987), and absolute magitude $M_V$, calculated as described in § 2. We also note the $V$ magnitude measured by the *HST* Snapshot observations, using the PC calibrations of Griffiths (1990), in cases where we could measure it and it differed by more than 0.2 mag from the tabulated value.

For two quasars, we have carried out ground-based CCD imaging in an attempt to identify the field of view. Exposures of 5–20 minutes through Johnson $V$ and Thuan-Gunn $I$ filters were obtained at the Palomar 1.5 telescope on the night of 1991 February 15. These observations confirmed that a targeted quasar (1613.7+715) was in the field of view in one *HST* exposure, and that a second quasar (1039+81) was missed in one of its exposures. The results are described in more detail below in § 5.1, Notes on Individual Objects.

Each of the quasar exposures was examined by eye for evidence of multiple images, the results being calibrated by simulations described below. We did not attempt more sophisticated detection methods such as deconvolution or point-spread function (PSF) subtraction. Such methods require detailed knowledge of the PSF and data with a high signal-to-noise ratio. In addition to the usual problems with the *HST* PSF, which varies strongly across the field of view (Burrows et al. 1991; Holtzman et al. 1991), each exposure has a different trailing direction and rate. There are usually no bright stars in the image with which the trailed PSF can be determined well, and the trail is often curved and/or uneven.

To determine the limits of detection of multiple images, we have carried out a series of tests. First, the trailed image of a bright star from one of the exposures having a typical drift rate (4.6 mas $s^{-1}$) was manually cleaned of cosmic-ray hits and scaled down so as to have 120,000 counts (i.e., photoelectrons) inside a 60 pixel (2''.6) radius. This corresponds, in the 230 s exposures, to a $V = 18.6$ object observed through the $V$ filter, or a $V = 18$ quasar observed through the $I$ filter. In the 120 s

TABLE 5

Maximum Detectable Magnitude Difference

| Separation | Position Angle of Second Image Relative to Trail Direction | | |
|---|---|---|---|
| | 0° | 45° | 90° |
| 0″12......... | ... | 1.0 | 1.5 |
| 0.16......... | 0.0 | 1.5 | 2.0 |
| 0.2.......... | 0.5 | 1.5 | 2.0 |
| 0.3.......... | 1.5 | 2.0 | 2.5 |
| 0.4.......... | 2.0 | 2.5 | 2.5 |
| 0.5.......... | 2.5 | 2.5 | 2.5 |
| 0.6.......... | 2.5 | 2.5 | 2.5 |
| 0.8.......... | 2.5 | 3.0 | 3.0 |
| 1.0.......... | 3.0 | 3.0 | 3.0 |
| 1.5.......... | 3.0 | 3.0 | 3.0 |
| 2.0.......... | 3.5 | 3.5 | 3.5 |

exposures, this number of counts would be obtained from a $V = 17.9$ object through the $V$ filter, or a $V \approx 17.2$ quasar through the $I$ filter. These magnitudes are representative of those of the fainter quasars that were observed. A secondary image, a scaled version of the PSF, was then added with a grid of separations from the primary image, of position angles relative to the trail direction, and of magnitude differences. Simulated readout noise and Poisson noise were added to the simulated image, and in some cases charged-particle events, taken from a real image, were also added. For each separation and position angle, the maximum magnitude difference for which the secondary image was discernible was noted. The results of these simulations are summarized in Table 5. The lower right-hand panel of Figure 2 shows one such simulated image.

To examine the objectivity of this test, the same procedure was carried out in a blind fashion, with a secondary image placed at random 0″–4″ from the primary. The brightness of the primary was also varied from 300,000 to 7700 counts. In some instances, no secondary images were added. Although the parameter space was covered less densely in the blind simulations, their results are consistent with the simulations described in the previous paragraph.

From Table 5, one can see that our survey is sensitive to the detection of multiple images at separations that have not been probed before. There is, however, a clear dependence of the detection limit at small separations on the position angle of the secondary image relative to the trail direction. "False" secondary images also appear sometimes at separations of $\approx 0\farcs2$, resulting from the trailing of the rings and the spokes in the PSF (see Holtzman et al. 1991). These artifacts can, however, be identified as such through their trail width, which is larger than that of a point source.

The flux limit of the images, as determined from the simulations, is about 3000 counts, corresponding to $V = 22.6$ in the 230 s exposures and $V = 22$ in the 120 s exposures through the $V$ filter. These brief exposures thus probe somewhat deeper than the Palomar Sky Survey. The $I$ exposures, in particular, often show many faint red objects which are invisible on the Palomar Sky Survey plates.

Returning to the observed quasars, in only two cases, 4C 56.28 and 1621+392, have we found additional sources near the quasar. Both of these observed configurations appear to involve chance superpositions, rather than cases of gravitational lensing. For these and several other objects, we make below some supplementary notes to Table 3.

### 5.1. *Notes on Individual Objects*

*0014+81.*—This is one of the most luminous quasars known and has previously been searched for evidence of lensing using ground-based optical imaging, VLA, and VLBI, with negative results (Kuhr et al. 1983, 1986). The first $I$ exposure of this quasar (which was among the first Snapshot exposures we received) seemed to show a faint secondary trail at 0″15 separation. Guided $I$ and $V$ exposures were obtained in 1990 November and 1991 January (see Table 1), to check the suggested structure. The $V$ exposure missed the target, but the successful $I$ exposure revealed no structure, indicating the faint trail previously seen resulted from a trailed feature in the halo of the PSF at the particular location in the field of view. We have subsequently seen similar effects in the trailed images of other quasars and stars in the PC and now recognize them as PSF artifacts.

*0506−61.*—The quasar appears 1 mag brighter in the January 9 $V$ exposure than in the October 3 $V$ exposure. (Both $I$ exposures were missed.) In January 9 it had $V = 17.4$, similar to the value measured by Adam (1978), and fainter than the $V = 16.8$ measured by Monk et al. (1986). Apparently, this is a highly variable quasar.

*0743−67.*—The quasar is in the field of view in all five exposures of this object. The trailing direction in the second $V$ exposure is at about 70° to the direction in the first and third $V$ exposures.

*1039+81.*—The October $V$ and $I$ exposures show an 18 mag object on PC-6, the $V$ exposure showing an additional, fainter object on PC-5 at a separation of 58″5. Neither the Palomar Sky Survey nor our CCD images from the Palomar 1.5 m telescope show such an object at this separation from the quasar. The $I$ exposure taken in March shows a 17 mag object on PC-6, plus a very faint, possibly diffuse source on PC-8, at 73″3 separation, which appears neither on the Palomar Sky Survey nor on our 1.5 m images. The $V$ exposure taken 11 days later has the quasar on PC-7 (two other stars in the field are identified), with $V = 18$. Thus it appears that the quasar was missed in the first and third exposures, and the identification is uncertain in the second exposure.

*1613.7+1715.*—The $I$ exposure of this quasar shows an object on PC-5 at 44″6 separation, not visible on the Palomar Sky Survey. However, our Palomar 1.5 m telescope CCD images clearly show a red object at that separation from the quasar, confirming that the object in the exposure on PC-7 is indeed the quasar.

*1621+392.*—The $V$ exposure of this quasar missed the target. However, the $I$ exposure shows additional point sources 7″2 northwest (position angle 317°) and 3″5 east (position angle 110°) of the quasar. An additional faint trail may be present 1″6 southeast (position angle 132°) of the quasar, but it is near our detection limit and may be a PSF artifact. The Palomar Sky Survey shows a number of other faint compact objects within several arcminutes of the quasar.

We have carried out spectroscopy for the quasar and the 3″5 east component. (This component is visible in Fig. 2, to the right of the quasar). The observation was carried out on 1991 April 5, at the Palomar 5 m Hale telescope using the 4-Shooter CCD camera/spectrograph (Gunn et al. 1987). The spectral range was 4500–9500 Å with a resolution of 25 Å. With the redshift of 1.97, the C IV $\lambda$1549, C III $\lambda$1909, and Mg II $\lambda$2800 emission lines are clearly detected in the quasar spectrum. The secondary component shows a $V = 19.5$ G-type stellar spectrum. The familiar stellar lines, H$\beta$ and Mg I $\lambda$5183, are seen in absorption at redshifts of $0.003 \pm 0.005$ and $-0.0025 \pm 0.006$, respectively. This is therefore a foreground Galactic star and not a gravitationally lensed image or a distant galaxy.

*4C 56.28* (*1857+56*).—Crampton et al. (1989) classified this object as a candidate lensed quasar based on the presence of an object 2''.8 at position angle 115° from the quasar. Their measurements showed that the second component was redder, but this was uncertain due to the relatively large noise in their $B$-band measurement. They suggested that the second component could be a lensed quasar image superposed on the lensing galaxy. The VLA observations of Lonsdale & Barthel (1987) do not show any radio emission at this location, but the companion, which is about 2.5 mag fainter than the quasar, could be below their detection limit. Unfortunately, the HST $V$ exposure missed the target, so a color comparison between the two objects cannot be made. However, the succesful $I$ exposure does not show any extended structure in the second component (see Fig. 2), suggesting it is not a galaxy.

## 6. DISCUSSION

### 6.1. *The Observed Lensing Frequency*

The 89 PC exposures we have obtained to date have resulted in high-resolution images of about 30 high-luminosity quasars. In the following calculations we will assume that we have observed 32 quasars. None of these show evidence of multiple imaging by gravitational lensing. In two quasars, 4C 56.28 and 1621+392, there are additional objects at separations of 3''–7'' from the quasar, which could conceivably be galaxies amplifying the quasars through lensing. However, the stellar densities in these fields are such that these companion objects could well be chance superpositions of foreground stars.

To calculate the observed frequency of lensing in our sample, we must account for the five quasars which passed the sample selection criteria but were rejected due to their being known lens systems with planned *HST* observations (see § 2). Since our survey is sensitive not only to small image-separation lenses, but to the whole range of expected image separations (up to $\approx 6''$), the known lenses would have undoubtedly been rediscovered by our survey, had they been included. One of the known lensed quasars, 2237+0305, is known to be quasar only because it is lensed; the object was found in a survey of bright nearby spiral galaxies (Huchra et al. 1985). It should therefore not be included among the five. Another of the known lensed quasars, 0957+561, is lensed by the combined effects of a galaxy and two clusters (Young et al. 1981). However, even if it were lensed only by the galaxy, and as a result had a smaller image separation, we would still detect it. We may therefore count four of the five known quasars as if they had been included in the sample and detected. Since we observed only 32 quasars out of the total sample of 354 quasars, we can assume that we have detected $32/354 \times 4 \approx 0.4$ cases of lensing. The detection of 0.4 or less cases of multiple images in 32 quasars rules out, at 95% confidence or better, scenarios in which more than $\approx 12\%$ of the quasars in our sample have multiple images in our detection range (see Table 5).

### 6.2. *Comparison to Theoretical Predictions*

Recent theoretical lensing models (e.g., FT) predict the lensing detection frequencies in several quasar samples. To predict the lensing detection frequency of the Snapshot Survey, we calculate for each quasar in our observed sample the optical depth to lensing $\tau$ and the amplification bias factor $B$.

$\tau(z)$ is the probability that a quasar at redshift $z$ will be lensed into multiple images by an intervening galaxy. Following TOG and Turner (1990), we assume an unevolving population of galaxies modeled as singular isothermal spheres (SIS) for which

$$\begin{aligned} \tau &= \frac{F}{4(y^2-1)^2}\left[(y^4+4y^2+1)\ln y - \frac{3}{2}(y^4-1)\right] && (\Omega_0 = 0)\,, \\ \tau &= \frac{4F}{15}(1-y^{-1/2})^3 && (\Omega_0 = 1)\,, \quad (3) \\ \tau &= \frac{F}{30}z^3 && (\Omega_0 = 0, \Lambda = 1)\,, \end{aligned}$$

where $y = z + 1$, $\Lambda$ is the cosmological constant, and $F$ is a dimensionless parameter proportional to the lensing effectiveness. Following FT, we assume $F = 0.045$.

The amplification bias $B(M_B, z)$ is the factor by which lensed quasars are overrepresented among quasars having absolute $B$ magnitude $M_B$ at redshift $z$, due to the apparent magnification of fainter lensed quasars to this brightness:

$$B(M_B, z) = \left[\tau(z)\int_0^\infty \phi(M_B+\Delta, z)P(\Delta)d\Delta\right]/[\tau(z)\phi(M_B, z)]\,. \quad (4)$$

Here $\phi(M_B, z)$ is the quasar luminosity function, giving the number density of quasars having $M_B$ at redshift $z$, and $P(\Delta)d\Delta$ is the probability that a multiple lensing event will increase the total flux from a quasar by $\Delta$ magnitudes. From Boyle et al. (1987), we take

$$\phi(M_B, z) = \phi^* \times 10^{0.4[M^*(z)-M_B](\beta+1)}\,, \quad (5)$$

with their best-fit parameters of $\beta = -3.6$ for $M_B \le M^*$, and $\beta = -1.2$ for $M_B \ge M^*$. $M^*(z)$ is the absolute magnitude of the break in the luminosity function and is given, for $H_0 = 50$ km s$^{-1}$ Mpc$^{-1}$ and $q_0 = 0.5$, by

$$M^*(z) = -2.5k_L \log(1+z) + M_0^*\,, \quad (6)$$

where $k_L = 3.5$ and $M_0^* = -21.75$. $\phi^*$ is a normalization that cancels out in equation (4), as does $\tau(z)$. We assume that this luminosity function, which was determined for $z < 2.2$, holds also for the higher redshifts of 10 of the quasars in our sample. Following TOG and FT, we assume an amplification probability describing amplification of a point source by a SIS:

$$P(\Delta)d\Delta = 7.37 \times 10^{-0.8\Delta}d\Delta\,, \qquad \Delta \ge 0.75\,. \quad (7)$$

Evaluating (4), we obtain:

$$B(M_B, z) = \begin{cases} 17.79 \times 10^{0.24(M^*-M_B)} - 20.14 & M_B \le M^* - 0.75 \\ 1.28 \times 10^{0.96(M^*-M_B)} & M^* - 0.75 \le M_B \le M^* \\ 1.28 & M_B \ge M^* \end{cases} \quad (8)$$

Note that although $B(M_B, z)$ was calculated for a certain choice of cosmology, it depends only on the slopes $\beta$ of the luminosity function, and on the difference $(M^* - M_B)$. As all of these are independent of cosmology, so is $B$. Note also that this $B$ differs from that calculated by FT, who approximated $B$ to be independent of redshift.

The expected number of lensed quasars in our sample is

$$N_{\mathrm{exp}} = 0.5 \sum \tau(z) B(M_B, z) , \tag{9}$$

the sum being over the 32 quasars observed. The factor of 0.5 is a correction to the SIS approximation that takes account of the finite core radii of the lensing galaxies (FT; see, however, Kochanek 1991). Most of the quasars do not have measured $B$ magnitudes. We assume a typical $B - V = 0.2$ in the quasar rest frame. To obtain $M_B$, we therefore add 0.2 mag to the values of $M_V$ in Table 4 and subtract 1.5 mag to transform from $H_0 = 100$ to the value of $H_0 = 50$ assumed by Boyle et al. (1987). Note that some of the quasars have varied by up to 2 mag (or were originally measured inaccurately). Quasar variability is obviously a further complication in the calculation of amplification bias and lensing probabilities. We use here the original Véron-Cetty and Véron (1987) $V$ values. We find

$$N_{\mathrm{exp}} = \begin{cases} 0.6 , & (\Omega_0 = 0, \Lambda = 0) \\ 0.3 , & (\Omega_0 = 1, \Lambda = 0) \\ 4.2 , & (\Omega_0 = 0, \Lambda = 1) \end{cases} \tag{10}$$

Among the allowed range of parameters of the luminosity function, the predicted number of lenses is most sensitive to $M_0^*$. Varying $M_0^*$ in the 1 $\sigma$ range given by Boyle et al. (1987) changes $N_{\mathrm{exp}}$ by $\approx \pm 50\%$.

As 4.2 quasars is $\approx 13\%$ of the present observed sample, under all the previous assumptions, we can formally reject a $\Lambda$-dominated universe at the 95% confidence level. However, this would be a rash step in view of all the uncertainties already outlined. Our results are nevertheless suggestive of low cosmological constant values, in accord with the conclusion reached by FT. As our sample is increased and the image quality is improved, we will be able to make a stronger test of these models.

### 6.3. *Comparison to Other Surveys*

Observationally, our results seem to be in conflict with those of Surdej (1989) who found that 23% of his sample was possibly lensed, and Crampton et al. (1989), who found the same fraction. Similarly, Webster et al. (1988) and Stocke et al. (1987) concluded that foreground galaxies are amplifying many quasars to within the detection limits of their surveys.

Some of the discrepancy may be explained by the fact that there are two different effects being studied: one is the splitting of a quasar into multiple images, and the other is the amplification of a quasar image. Webster et al. (1988) and Stocke et al. (1987) are mostly sensitive to the latter effect. Narayan (1989) and Kovner (1989) have pointed out that the effect Webster et al. see is in any case too large for any lensing explanation. Additionally, it is difficult to see how so much amplification could take place without some splitting of the quasar image by the galaxy potential.

Crampton et al. (1989) and Surdej (1989) are sensitive to both the existence of nearby galaxies and multiple images. Of the 32 quasars of Crampton et al., four have double images; two are within a few arcseconds of a galaxy; and one, 4C 56.28, observed by us as well, has a double image, but with probably different colors. They suggest that in 4C 56.28 the second image is again a galaxy that is amplifying the quasar, or a combination of a lensed image and a foreground galaxy. Assuming this explanation, they have seen galaxies in the vicinity of three of their quasars. In our sample, which is of comparable size and somewhat better detection sensitivity, we have seen objects in the vicinity of two quasars: 4C 56.28 and 1621+392. The statistics may therefore agree in the two samples, although we have shown that one of the companions to 1621+392 is a foreground star. Of the four double images reported by Crampton et al., the quasar 0747+61 shows some extended structure, but its image was obtained under poor seeing conditions, and the results are therefore inconclusive. This leaves three doubly imaged quasars in their sample, two of them with subarcsecond separations. When this is compared to the zero such cases we have found, the disagreement is not as large. As our sample is increased in the future, this question can be addressed more definitely.

A similar comparison with the survey of Surdej (1989) is difficult, since it does not report how many objects in the sample were multiple stellar images, how many were projected near a galaxy, and how many showed complex but not clearly distinguishable structure. Magain et al. (1989) did search for an overlying galaxy in 83 quasars from the Surdej sample by subtracting a point-spread function from the quasar image. They found galaxies in three cases with multiple quasar images in two of these. Finally, Surdej (1989) also reports that five of the 111 quasars in the sample are excellent lens candidates. If this is taken as the actual number of multiply lensed objects they found, then a $\approx 5\%$ fraction of multiple imaging is implied both by their results and those of Crampton et al. (1989). Our results are still consistent with such a fraction, although, if it is truly this large, we should soon discover some multiply imaged quasars.

### 6.4. *Implications of Engineering Results*

The absence of the stellar aberration correction when *HST* is operated in gyro mode has important consequences for the efficiency of the observatory. In normal slewing from target to target, the resulting initial large pointing error requires more time to find guide stars.

There are indications that the intrinsic gyro drift rate in the absence of stellar aberration may be small. For example, on the March 1 $V$ exposure of 0348+06, for which the target direction was nearly perpendicular to the spacecraft's orbital velocity, the drift rate was only 0.6 mas $s^{-1}$, i.e., the trail was only 3 pixels, or 0".13 long. Although some chance cancellation of errors may have been involved in this particular example, an intrinsic drift rate this small could also be important for the observatory's performance. For example, short exposures of a duration of few minutes may be taken effectively using only gyro guiding; the time required for acquiring guide stars would then be saved.

## 7. SUMMARY

We have reported on the first results from the *HST* Non-Proprietary Snapshot Survey. None of the approximately 30 quasars we have observed at high spatial resolution show evidence of multiple imaging by gravitational lensing. We have not encountered the high occurrence rate of multiple imaging at surbarcsecond separations reported by several ground-based surveys, notably Crampton et al. (1989) and Surdej (1989). This is surprising in view of the fact that the high spatial resolution of *HST* would have detected such cases had they occured. While our statistics are still low enough such that our results are not significantly in conflict with those surveys, our continuing observations will provide a strong test of the relatively high incidence of lensing.

Our observations so far indicate that gravitational lensing is a rare phenomenon, and that not a large fraction of lenses are "hiding" at small image separations. This rarity of lensing supports the idea that we do not live in a universe dominated by a cosmological constant.

From the engineering aspect, this program has helped uncover several software problems in the observatory's operation. Most importantly, we have found that the lack of correction for stellar aberration when the telescope is in gyro mode causes much of the large pointing errors and the long trailed images obtained when solely under gyro control. Correction of this problem may reduce the overhead time required in Fine-Guidance-Sensor guided observations for the acquisition of guide stars, and may also make brief gyro-guided observations attractive to other observers. We will continue monitoring the gyro performance throughout Cycle 1 of observations (until 1992 June).

Since the Snapshot Survey is not a standard observing program, its implementation required imaginative approaches by a number of individuals at the Space Telescope Science Institute, all of whom were enthusiastic about the idea of using *HST* when it could not be scheduled for approved science programs. We are grateful to R. Giacconi for deciding to try out this idea on Director's discretionary time; to P. Stockman and D. Macchetto, who set the guidelines for the operation of the project; to A. Saha, B. Whitmore, and the SPSS operations staff, who guided the project through an unconventional scheduling maze; and to L. Petro and O. Richter, who took reponsibility for overseeing the survey at STScI. We are grateful to J. Gunn for the original suggestion that we observe quasars and for much technical advice during the planning stages; to B. Wills for generously supplying a number of unpublished finding charts; to H. Netzer, N. Brosch, and A. Almoznino for obtaining at the Wise Observatory contemporary photometry for several of the quasars we observed; to M. Schmidt for obtaining at Palomar Observatory a spectrum of one of the quasars; to E. Turner and R. Romani for stimulating and informative discussions; and to C. Kochanek for suggesting several important improvements to the original manuscript. This work was supported by NASA grant NAS5-29225 (J. N. B., N. A. B., and D. P. S.), Space Telescope Science Institute grant GO-2775.01 (D. M.), and a Hubble Space Telescope Fellowship HF-1013.01-90A (B. Y.).

## REFERENCES

Adam, G. 1978, A&AS, 31, 151
Bennett, C. L., Lawrence, C. R., Burke, B. F., Hewitt, J. N., & Mahoney, J. 1984, ApJS, 61, 1
Boyle, B. J., Fong, R., Shanks, T., & Peterson, B. A. 1987, MNRAS, 227, 717
Burrows, C. J., Holtzman, J. A., Faber, S. M., Bely, P. Y., Hasan, H., Lynds, C. R., & Schroeder, D. 1991, ApJ, 369, L21
Crampton, D., McClure, R. D., Fletcher, J. M., & Hutchings, J. B. 1989, AJ, 98, 1188
de Vaucouleurs, G., de Vaucouleurs, A., & Corwin, H. G. 1976, Second Reference Catalog of Bright Galaxies (Austin: University of Texas Press)
Fugmann, W. 1988, A&A, 204, 73
Fukugita, M., Futamese, T., & Kasai, M. 1990, MNRAS, 246, 25P
Fukugita, M., Futamese, T., Kasai, M., & Turner, E. 1991, preprint
Fukugita, M., & Turner, E. L. 1991, MNRAS, 253, 99 (FT)
Gott, J. R., Park, M. G., & Lee, M. H. 1989, ApJ, 338, 1
Griffiths, R. 1990, WF/PC Instrument Handbook (Baltimore: Space Telescope Science Institute)
Gunn, J. E., et al. 1987, Opt. Engineering, 26, 779
Hewitt, A., & Burbidge, G. 1989, ApJ, 69, 1
Holtzman, J. A., et al. 1991, ApJ, 369, L35
Huchra, J., Gorenstein, M., Kent, S., Shapiro, I., Smith, G., Horine, E., & Perley, R. 1985, AJ, 90, 691
Jauncey, D. L., et al. 1989, AJ, 98, 54
Kochanek, C. S. 1991, ApJ, 379, 517
Kovner, I. 1989, ApJ, 341, L1
Kuhr, H., Liebert, J. W., Strittmatter, P. A., Schmidt, G. D., & Mackay, C. 1983, ApJ, 275, L33
Kuhr, H., et al. 1986, ApJ, 302, 52
Lahav, O., Lilje, P. B., Primack, J. R., & Rees, M. J. 1991, MNRAS, 251, 128
Lonsdale, C. J., & Barthel, P. D. 1987, AJ, 94, 1487
Magain, P., Remy, M., Surdej, J., & Swings, J. P. 1989, in Gravitational Lensing, ed. Y. Mellier, B. Fort, & G. Soucail (Berlin: Springer), 88
Meylan, G., & Djorgovski, S. 1989, ApJ, 338, L1
Monk, A. S., Penston, M. V., Pettini, M., & Blades, J. C. 1986, MNRAS, 222, 787
Narayan, R. 1989, ApJ, 339, L53
Schneider, D. P., Schmidt, M., & Gunn, J. E. 1991, AJ, in press
Stocke, J. T., Schneider, P., Morris, S. L., Gioia, I. M., Maccacaro, T., & Schild, R. E. 1987, ApJ, 315, L11
Surdej, J. 1989, in Gravitational Lensing, ed. Y. Mellier, B. Fort, & G. Soucail (Berlin: Springer), 88
Tritton, K. P. 1971, MNRAS, 155, 1P
Turner, E. L. 1990, ApJ, 365, L43
Turner, E. L., Ostriker, J. P., & Gott, J. R. 1984, ApJ, 284, 1 (TOG)
Véron-Cetty, M. P., & Véron, P. 1987, A Catalogue of Quasars and Active Nuclei (3d ed; Munich: ESO)
Webster, R. L., et al. 1988, Nature, 336, 358
Webster, R. L., Hewett, P. C., & Irwin, M. J. 1988, AJ, 95, 19
Young, P., Gunn, J. E., Kristian, J., Oke, J. B., & Westphal, J. A. 1981, ApJ, 244, 736